Electronic Supplementary Material (ESI) for Energy & Environmental Science.
This journal is © The Royal Society of Chemistry 2017

Electronic Supporting Information

Asymmetric Faradaic systems for selective electrochemical separations

Xiao Su[1], Kai-Jher Tan[1], Johannes Elbert[1], Christian Rüttiger[3], Markus Gallei[3],
Timothy F. Jamison[2] and T. Alan Hatton[*1]

Materials and Methods

All reagents were purchased from Sigma Aldrich and PolySciences without further purification unless otherwise noted. CpCoCb was synthesized according to literature. [1] All ^{1}H NMR was performed on a Varian 500 MHz, and the Physical Electronics Versaprobe II X-ray Photoelectron spectrometer was used for the analysis of the surface of the electrodes. The analysis was performed at ultra-high vacuum (10^{-8} bar) with an argon-gun neutralizer. All electrochemical studies were performed on a VersaSTAT 4 potentiostat (Princeton Applied Research) with automatic IR compensation between 50 MΩ and 5 Ω. The surface morphology of the electrodes were characterized by a FEG-XL-30 field-emission SEM at 20 kV using a beam size of 3 and high vacuum conditions for EDX, and a ZEISS Merlin High-Resolution SEM at 5kV-20 kV for the high resolution images in the main text.

1. Electrode Preparation

PVF-CNT (polyvinylferrocene-functionalized electrode):

The detailed preparation methods for the **PVF-CNT** electrodes are discussed in previous publications from our group.[2, 3] The base electrodes were prepared by cutting 2 cm by 1 cm swatches of Teflon-treated Toray carbon paper obtained from Electrochem Inc, then soldering them with copper tape and wire. The PVF/CNT electrodes were prepared by drop casting. A stock solution A of 80 mg poly(vinyl)ferrocene (PVF) (Polysciences, Inc) and 40 mg multiwalled-CNT (MWCNT, Sigma) was dissolved in 10 mL anhydrous chloroform. A stock solution B of 40 mg of CNT in 10 mL chloroform was also prepared. The two stock solutions were sonicated for 2 hrs in icy water to optimize dispersion level. The PVF/CNT(1:1) ratio was prepared by mixing stocks A and B in a 1:1 ratio: 1 mL of A was mixed with 1 mL of B and sonicated for another 3 hrs in an ice-bath, before drop-casting 50 μL, equivalent to a 1 drop PVF/CNT(1:1) and left to dry at 25^{o}C. For sorption experiments, a 1:1 mass ratio of PVF to CNT was used with 4 drops (resulting in 4 μmoles of ferrocene units). PVF/CNT(1:2) was prepared by combining different amounts of the two stock solutions. For all the systems, the immersed electrochemical area is equivalent to 1.2 cm^2 (1 cm by 1.2 cm).

$CoCp_2$-CNT-cp (Cobaltocenium-paste electrode):

20 mg of cobaltocenium hexaflourophosphate (Strem Chemicals, 98%), 20 mg of carbon paste (BASI Carbon Paste, Oil Base), and 10 mg of carbon nanotubes (Sigma-Aldrich, Multi-Walled, >95%) were added to 5 mL of chloroform (Sigma-Aldrich, 99.9%). The solution was sonicated in an ice bath for a minimum of 45 minutes, and then drop cast onto 1 cm x 2 cm strips of Teflon-treated carbon conductive paper (ElectroChem Incorporated, EC-TP1-060T), which had been brushed lightly 5-10 times on each side with a razorblade. A total of four 50 μL drops were drop cast onto each strip, with two drops on each side. The second drop on each side was drop cast only after the first drop had dried. Once the last of the drops finished drying, each strip was attached to a copper wire using conductive copper tape.

Rubpy-CNT-cp (Ruthenium-paste electrode):

40 mg of cis-Dichlorobis(2,2'-bipyridine)ruthenium(II) (Sigma-Aldrich, 97%) and 40 mg of carbon paste (BASI Carbon Paste, Oil Base) were added to 5 mL of N,N-Dimethylformamide (DMF) (Sigma-Aldrich, 99.9%) to form one solution, and 20 mg of carbon nanotubes (Sigma-Aldrich, Multi-Walled, >95%) was added to 5 mL of DMF to form a second solution. Both solutions were sonicated separately in a water bath at room temperature for a minimum of 45 minutes, before being combined and sonicated again in a water bath at room temperature for a minimum of 45 minutes. The solution was then drop cast onto 1 cm x 2 cm strips of Teflon-treated carbon conductive paper (ElectroChem Incorporated, EC-TP1-060T). A total of four 50 μL drops were drop cast at the same time onto one side of each strip. The strips were dried in a vacuum oven at 80^oC and -30mmHg for 3-4 minutes (until dry). Each strip was attached to a copper wire using conductive copper tape.

Potassium-ferricyanide (Potassium ferricyanide-paste electrode):

40 mg of potassium ferricyanide, 40 mg of carbon paste (BASI Carbon Paste, Oil Base) and 20 mg of CNT were mixed in a mortar and pestle, and 3 mg was pasted onto the surface onto a 1 cm x 2 cm strips of Teflon-treated carbon conductive paper (ElectroChem Incorporated, EC-TP1-060T). Two drops of chloroform were applied on top of the surface to smooth the surface. Each strip was attached to a copper wire using conductive copper tape. For the sodium ferrocyanide system, 80mg of sodium ferrocyanide, 20mg CNT, and 20mg carbon paste were mixed in 20mL DMF, sonicated for a minimum of 45 min and similar to the previous organometallics, drop-cast onto carbon fiber electrodes and dried in vacuum for 3-4 min.

$PMAECoCp_2$-CNT (cobaltocenium-polymer functionalized electrode):

Poly(2-(methacrylolyoxy)ethyl cobaltocenium) ($PMAECoCp_2$) was synthesized according to the procedures outlined below. 20 mg of $PMAECpCp_2$ and 10 mg of CNT were dispersed in 5 mL of DMSO by sonication for 45 min at room temperature. A total of 200 uL of solution was drop-cast onto 1 cm x 2 cm strips of Teflon coated-carbon paper for a 4-drop electrode. The strips were dried in a vacuum oven at 80^{o}C and -30mmHg for 3-4 minutes (until dry). Each strip was attached to a copper wire using conductive copper tape. Depending on the amount of PVF/CNT on the working electrode, the amount of PMAECoCp$_2$-CNT can be varied to match the charges on the electrodes. The PMAECoCp$_2$ electrodes were characterized accordingly by XPS and SEM.

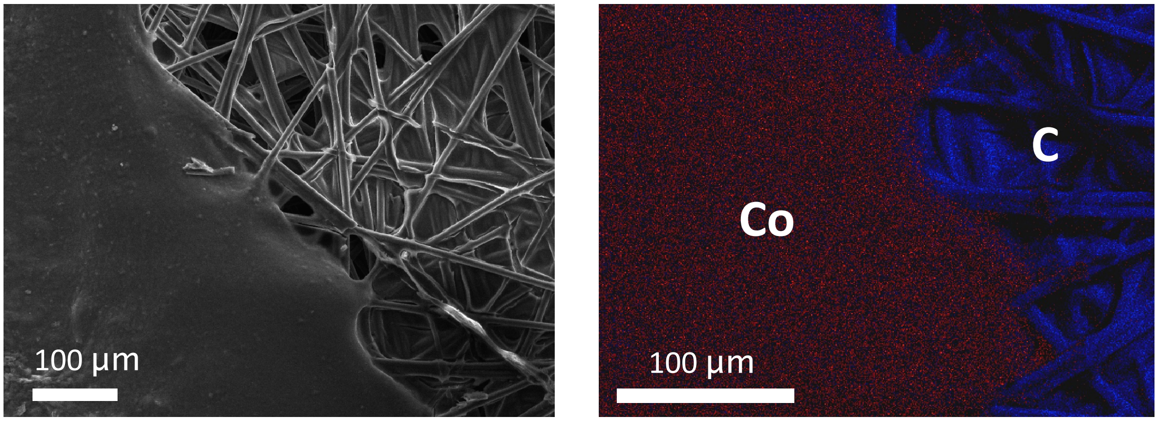

Figure 1.1. SEM and SEM-EDX of PMAECoCp$_2$-CNT coated on carbon paper fibers

PCpCoCbMA-CNT ((cyclopentadienyl)cobalt(tetraphenyl-cyclobutadiene)-polymer functionalized electrode):

16 mg of CNT were dispersed in 4 mL of chloroform by sonication for 45 min at 0°C. Then 16 mg poly[η^5-(1-oxo-4-methacryloyloxy-butyl)-cyclopentadienyl]cobalt(η^4-tetraphenylcyclobutadiene) (PCpCoCbMA) are added and the dispersion is sonicated for another 45 min. A total of 200 µL of solution was drop-cast onto 1 cm x 2 cm strips of Teflon coated-carbon paper for a 4-drop electrode. The strips were dried at room temperature. Each strip was attached to a copper wire using conductive copper tape.

2. Cobaltocenium Polymer Synthesis

The synthesis procedure for Poly(2-(methacrylolyoxy)ethyl cobaltocenium) (PMAECoCp$_2$) with a hexafluorophosphate counter-ion was adapted from literature.[4-6]

2.1. 2-(Methacrylolyoxy)ethyl cobaltocenium hexafluorophosphate (MAECoPF$_6$).

As opposed to following the acyl-chloride route previously reported,[5] mono-carboxylcobaltocenium was directly coupled with (hydroxyethyl)methacrylate (HEMA) using Steglich esterification. Mono-substituted carboxylcobaltocenium (1.2 g, 3.17 mmol) was dissolved with HEMA (0.62 g, 4.76 mmol) and N,N-dimethylamino pyridine (DMAP, 0.74 g, 6.02 mmol) in 30 ml anhydrous acetonitrile, A solution of N,N'-dicyclohexylcarbodiimide (DCC, 0.73 g, 3.52 mmol) in 10 ml acetonitrile was added slowly at 0°C. The mixture was then stirred at room temperature for 16 h. The reaction mixture was filtered to remove N,N'-dicyclohexylurea. The solution was diluted with Dichloromethan and subsequently washed with 1 M HCl, 1 M NaOH and water. The organic phase was dried with MgSO$_4$, filtered and concentrated under reduced pressure. MAECoPF$_6$ was precipitated by adding diethylether. The yellow product was filtered, washed with diethylether and dried under vacuum. Yield: 600 mg^{1}H NMR (D$_6$-DMSO, δ, ppm): 6.27 (t, 2H, Cp),6.22 (m, 1H, CH_2=C), 6.11 (t, 2H, Cp), 5.99 (s, 5H,Cp), 5.93 (m, 1H, CH_2=C), 4.54 (m, 2H, OCH_2CH$_2$O), 4.46 (m,2H, OCH$_2$CH_2O), 1.90 (m, 3H, CH_3).

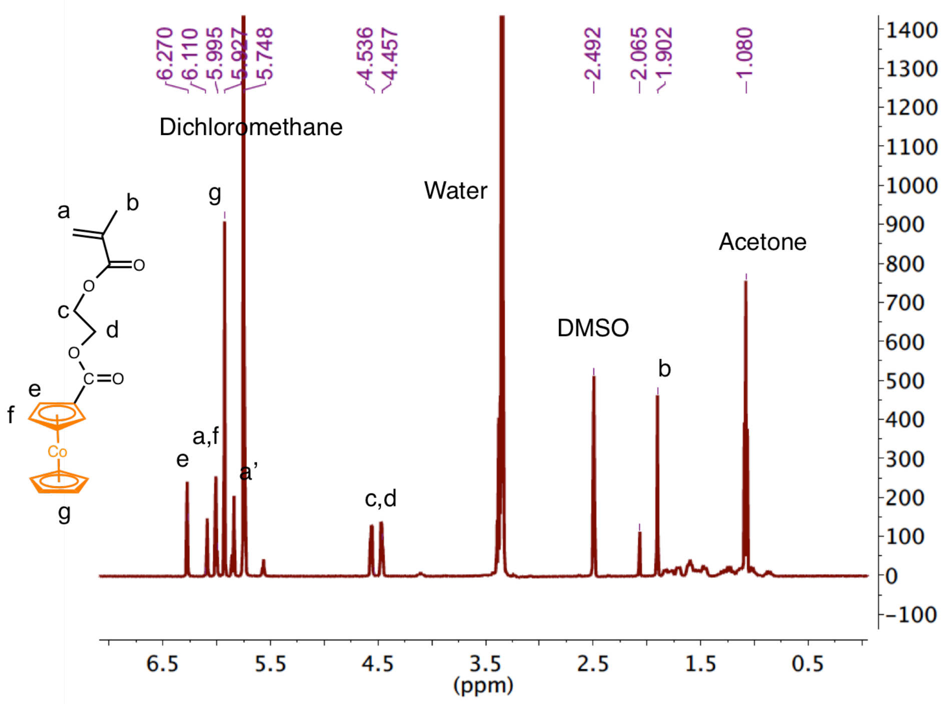

Figure S2.1. NMR spectra of synthesized monomer MAECoPF$_6$

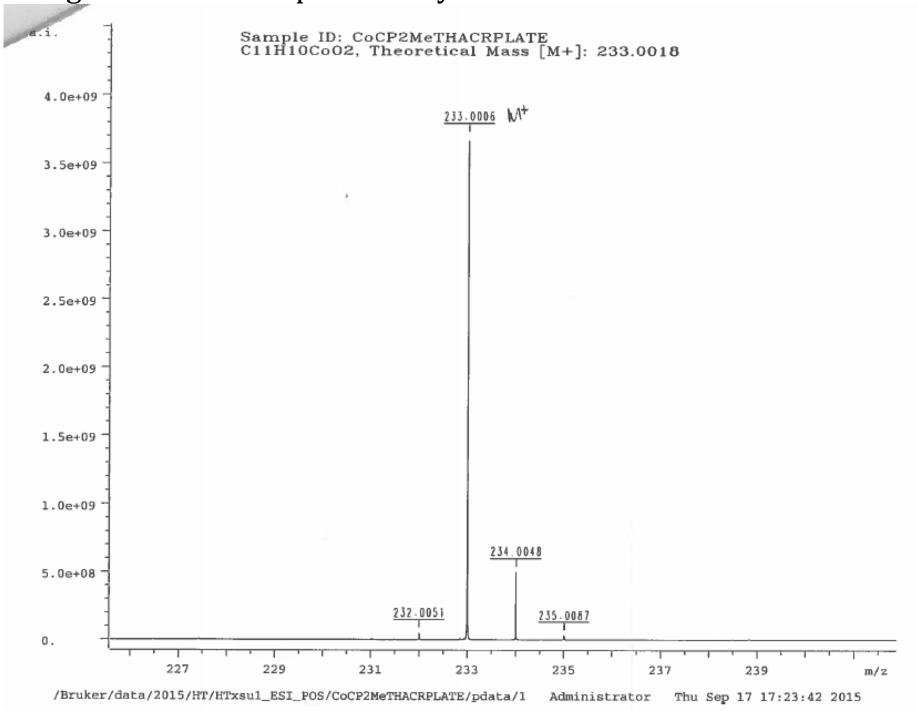

Figure S2.2. Cation-mass spectra for cation component of monomer MAECoPF$_6$ (233.0016).

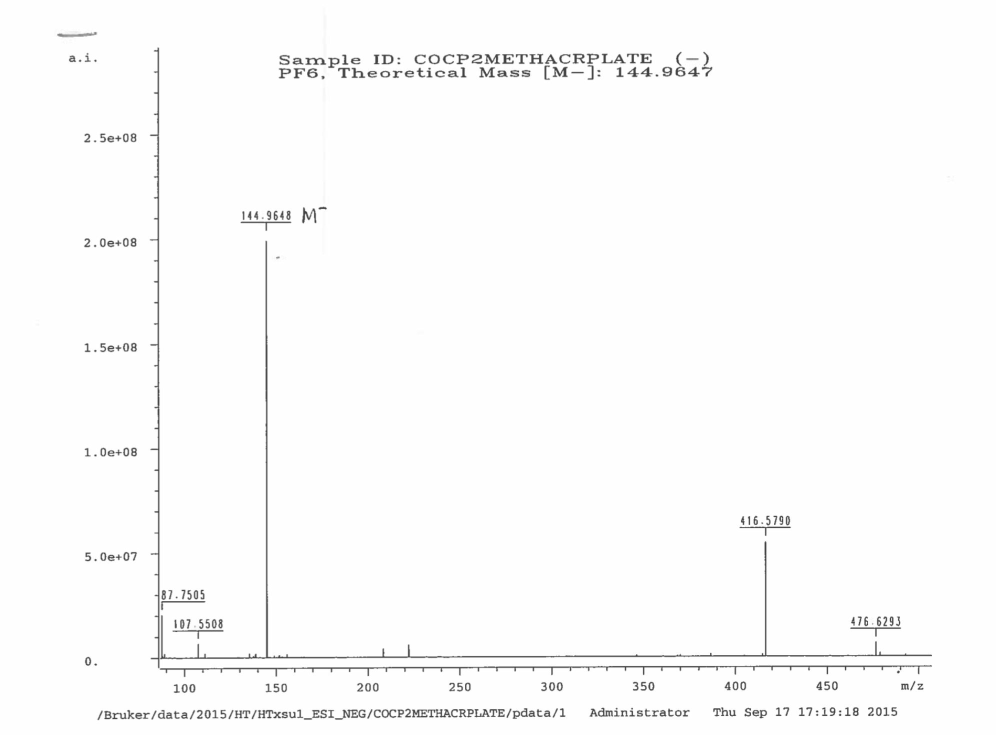

Figure S2.3. Anion-mass spectra showing PF$_6^-$ (144.698) as the main anion.

2.2. Free-radical polymerization of $MAECoPF_6$

The monomer $MAECoPF_6$ (300 mg, 0.61 mmol) and AIBN (1.97 mg, 0.012 mmol) were dissolved in 3 mL THF in a Schlenktube. The vessel was flushed with nitrogen, and the mixture was heated to 70°C for 20 hrs. The product was precipitated in 40 mL dichloromethane, and by centrifugation. The final average molecular weight was found to be 184200 g/mol using gel permeation chromatography (GPC) by comparing to PMMA standards.

2.3. Synthesis of PCpCoCbMA

PCpCoCbMA was synthesized according to previously published literature procedures.[7] The free radical polymerization of [η^5-(1-carboxy-propylmethacrylate)-cyclopentadienyl]cobalt(η^4-tetraphenylcyclobutadiene) is described below.

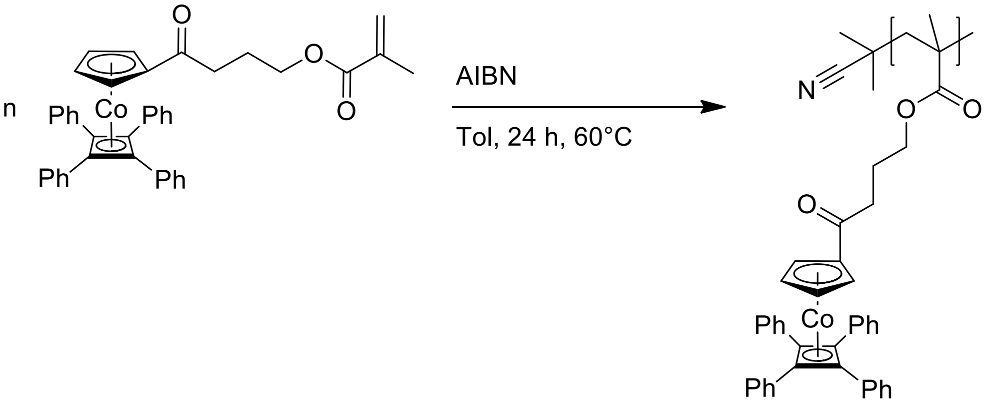

Figure S2.4. Free-radical polymerization scheme of CpCoCbMA to result in PCpCoCbMA

The cobalt-containing methacrylate CpCoCbMA (500 mg, 0.8 mmol, 1 equiv.) was dissolved in a solution of AIBN (13.15 mg, 0.08 mmol) in toluene (3.25 mL) and stirred for 24 hours at 60°C. The polymer was precipitated in 50 mL methanol, collected by centrifugation, dissolved in DCM and precipitated in methanol again. The obtained polymer was dried in vacuum yielding a yellow solid (60 mg, 12 %).
M_n: 8900 g mol^{-1}, M_w: 18600 g mol^{-1}, PDI: 2.09 (SEC vs. PS standards)
M_w: 56000 g mol^{-1} g mol^{-1} (SEC-MALLS)
^1H NMR (300.0 MHz, $CDCl_3$): δ 7.40 (b, 8 H; Ph); 7.12 (b, 12 H; Ph); 5.11 (b, 2 H; Cp); 4.61 (b, 2 H; Cp); 3.60 (b, 2 H; CH_2); 1.88 (b, 2 H; CH_2); 1.42 (b, 2 H; CH_2); 0.78 ppm (b, 3 H; α-CH_3)

3. Electrochemical Characterization and Parameters

Table 3.1. Table of reduction potentials for the heterogeneous-redox functionalized electrodes) in 100 mM $LiClO_4$.

Redox organometallic	**$E_{red, ½}$ vs Ag/AgCl in 100 mM $LiClO_4$ (25°C)**
PVF^+-CNT	+0.12 V
$Rubpy^+$-CNT-cp	+0.18 V
$Fecy^+$-CNT-cp	+0.15 V
$PMMAECoCp_2^+$-CNT	-0.8 V
PCoCpCbMA-CNT	-0.45 V
Water reduction	**-1.1 V**

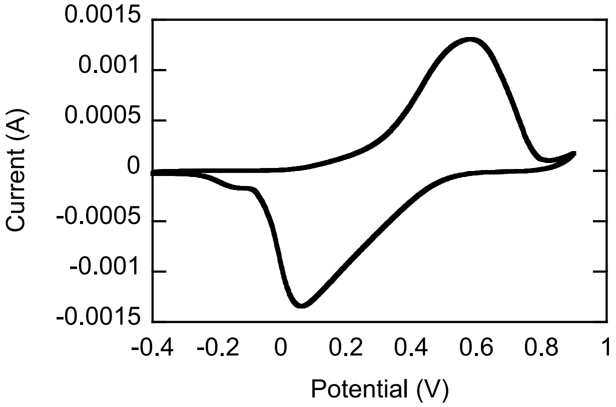

Figure 3.1. Cyclic voltammogram of PVF-CNT at 0.1 M $LiClO_4$ at 0.005 V/s

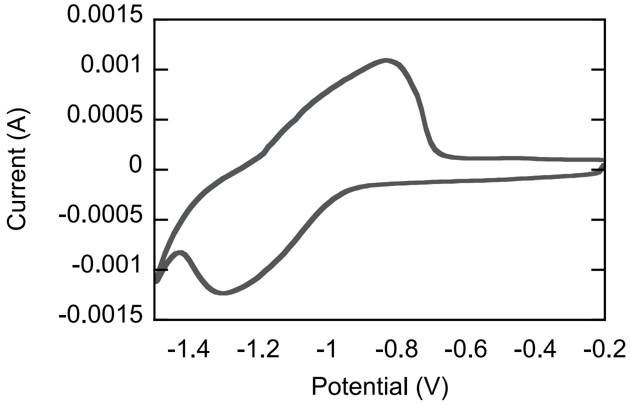

Figure 3.2. Cyclic voltammogram of $CoCp_2$-CNT-cp at 0.1 M $LiClO_4$ at 0.01 V/s.

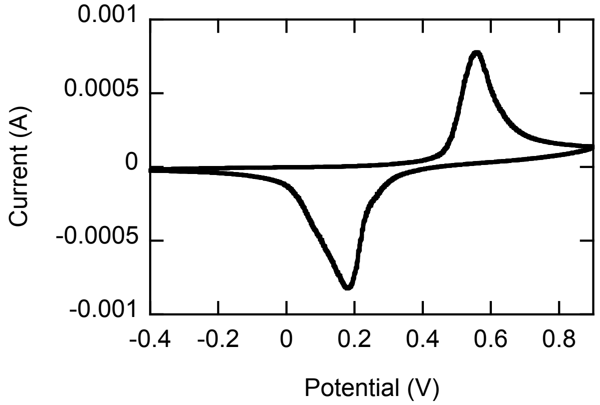

Figure 3.3. Cyclic voltammogram of on Rubpy-CNT-cp at 0.1 M $LiClO_4$ vs Pt at 0.01 V/s.

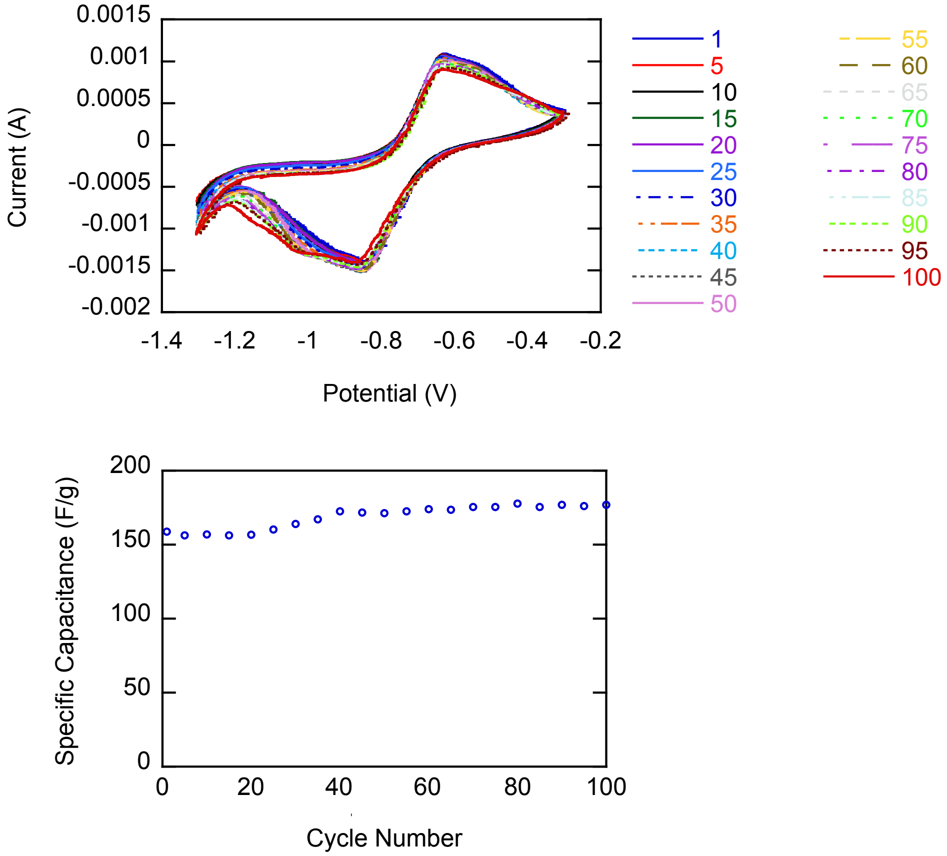

Figure 3.4. Charge Stability of $PMAECoCp_2$-CNT at Left) 0.005 V/s in 0.1 M $LiClO_4$ with Pt as counter, Ag/AgCl reference and Right) specific capacitance from the area of the CVs on the left.

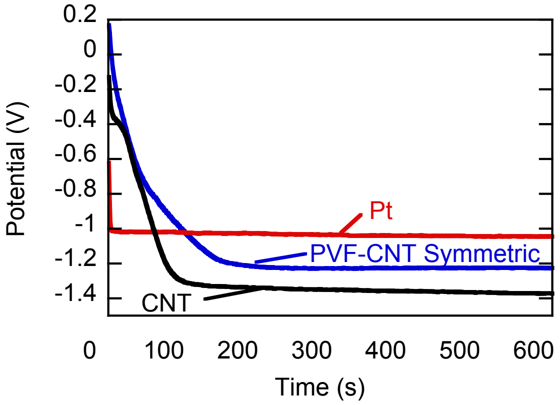

Figure 3.5. Charging of various capacitive counter-cathode with PVF-CNT as the anode counter at (at -0.83 A/m^2). Tracking the redox potential of the cathode allows us to see the onset of water reduction.

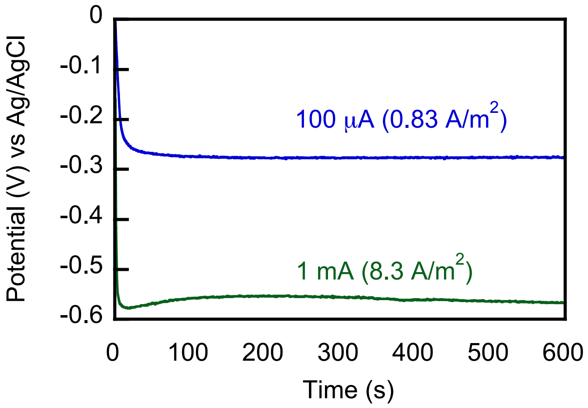

Figure 3.6. Charging of PMAECoCp$_2$ with PVF-CNT as the anode counter at two different current densities (-0.83 A/m^2 and -0.83 A/m^2).

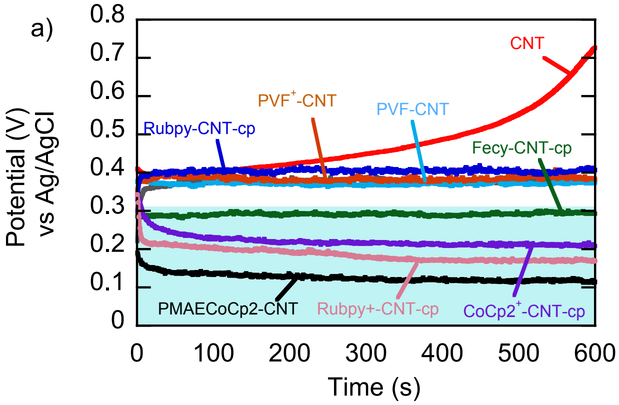

Figure 3.7. Potential applied on anode under chronopotentiometry (100 μA) over 10 min for various counter-electrode materials when operating with PVF-CNT as the working electrode in three-electrode configuration.

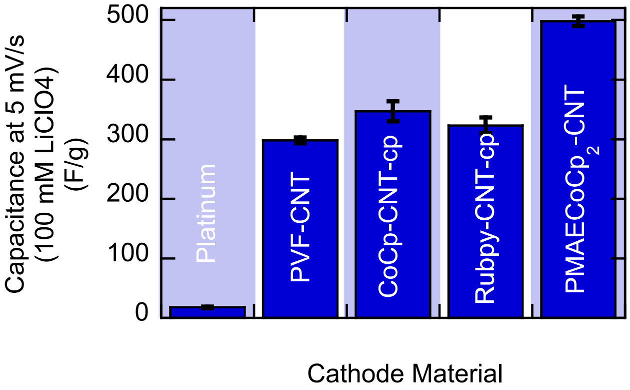

Figure 3.8. Specific capacitance from three-electrode CV of PVF-CNT working anode combined with various cathode materials being tested in the current work. The immobilized cobaltocenium-polymer counter ($PMAECoCp_2^+$-CNT) was the counter-electrode screened yielding the highest relative specific capacitance for the system.

4. pH tests and capacitance calculations

The pH tests were conducted with an in-situ pH probe (Thermo Scientific Orion pH Probe) placed in the solution through a modified 4 entrance cell top. All pH tests, unless otherwise stated, were carried out using 0.1 M $LiClO_4$ in 6 mL deionized water (MiliQ). Moderate constant stirring of the solution was effected throughout each test with the placement of a small stir bar in the center of the cell. The electrodes and pH probe were positioned at a constant submerged depth and in a manner to avoid physical interference from the stir bar. Nitrogen purge was maintained during the entire hydroxide formation test. Prior to starting each test, nitrogen was bubbled through the solution until pH equilibrium was reached, after which the nitrogen purge tip was lifted to maintain the purge above the solution. After the equilibrium pH readings with purge tip inside and above the solution were taken, the test was started and the pH reading was measured every 10 seconds thereafter.

The obtained pH readings were then converted to yield the amount of charge used to produce hydroxide ions through water splitting, as follows:

Converting pH to moles:

$$n_{OH^-\,produced}(t) = V_{solution}\left(\left(10^{-(14-pH(t))}\right) - \left(10^{-(14-pH(t=0))}\right)\right)$$

Converting moles to charge through Faraday's laws of electrolysis:

$$Q_{OH^-\,produced}(t) = n_{OH^-\,produced}(t) * F * z_{OH^-}$$

The electrochemical capacitances for the single electrodes ($PMMAECoCp_2$ and PVF-CNT) were performed by integrating CVs areas and a scan-rate at 5 mV/s in 100 mM $LiClO_4$ with Pt as the counter, and using the mass of the active organometallics + CNT as the specific value $C = \frac{\int i(E)dE}{v(E_2-E_1)} \cdot \frac{1}{m_{electrode}}$. $E_2 - E_1$is the potential window, with v being the scan-rate. For the combined asymmetric systems, PVF-CNT was maintained as the working anode, and the various electrodes with varying redox-organometallics were used as the counter-cathodes $C = \frac{\int i(E)dE}{v(E_2-E_1)} \cdot \frac{2}{(m_{PVF-CNT}+m_{counter})}$, with again the masses including both PVF, CNT and any binder.

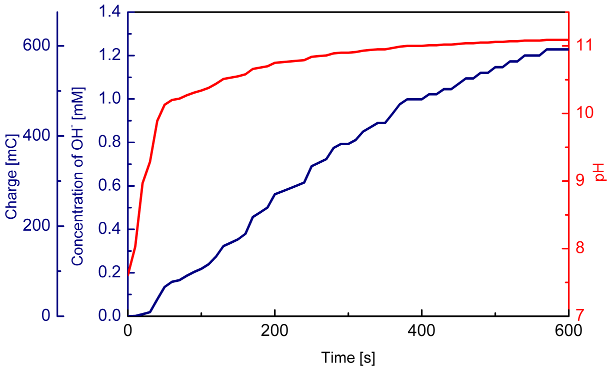

Figure 4.1. pH vs charge vs concentration of OH- of model PVF-CNT electrode with Pt counter over 600 s chronoamperometry (8.3 A/m^2)

5. Hydroxide production results of PVF-CNT//Pt configuration at varying concentrations of electrolyte.

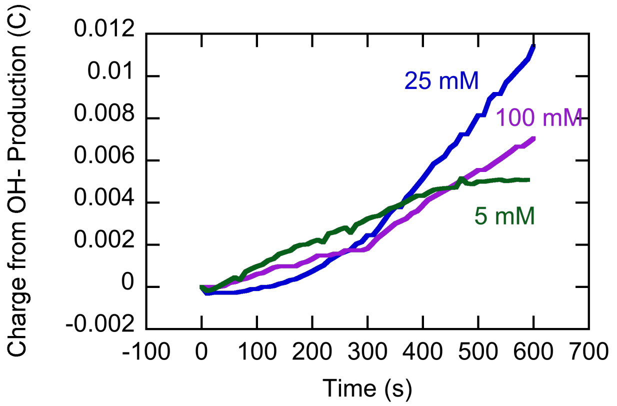

Figure 5.1. OH- production from PVF-CNT//Pt at various electrolyte concentrations using chronopotentiometry (+100 μA).

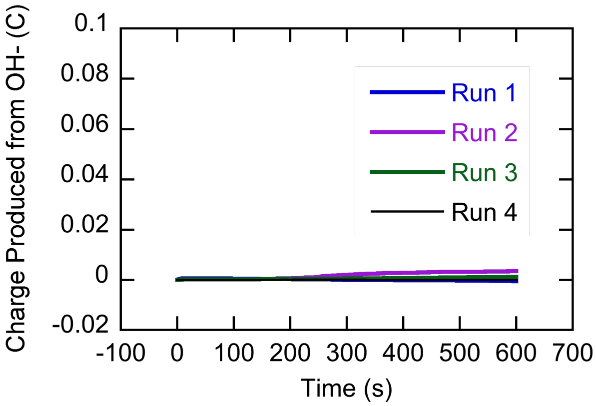

Figure 5.2. PVF-CNT//CoCp⁺-CNT-cp at different $LiClO_4$ concentrations under at 100 μA chronopotentiometry: 5 mM (green), 25 mM (blue), 100 mM (green), 100 mM repeat (black).

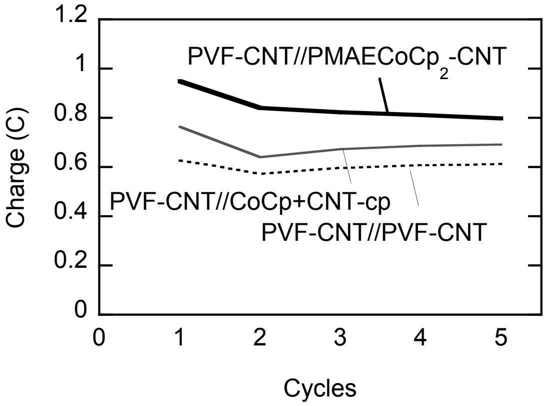

Figure 5.3. Comparison of electrochemical charge storage of system with PVF//CNT as working electrode in 3-electrode cell configuration, obtained through CV for a 1.2 V range in 0.005 V/s in 100 mM $LiClO_4$.

XPS Spectroscopy for Cobaltocenium-Electrodes

Physical Electronics Versaproble II X-ray Photoelectron spectrometer was used for the analysis of the surface of the electrodes. The analysis was performed at ultra-high vacuum (10^{-8} bar) with an argon-gun neutralizer. The survey runs were performed with 10 cycles from 1400 eV to 50 eV at 200 kV with a pass energy of 80 eV and a step size of 0.5 eV. The high resolution scans for were performed with 100 kV, a pass energy of 11 eV, 0.05 eV resolution with 30 cycles for iron and 8 cycles for the remaining elements. The scans were exported using CASA XPS commercial software (MIT license) and MULTIPAK.

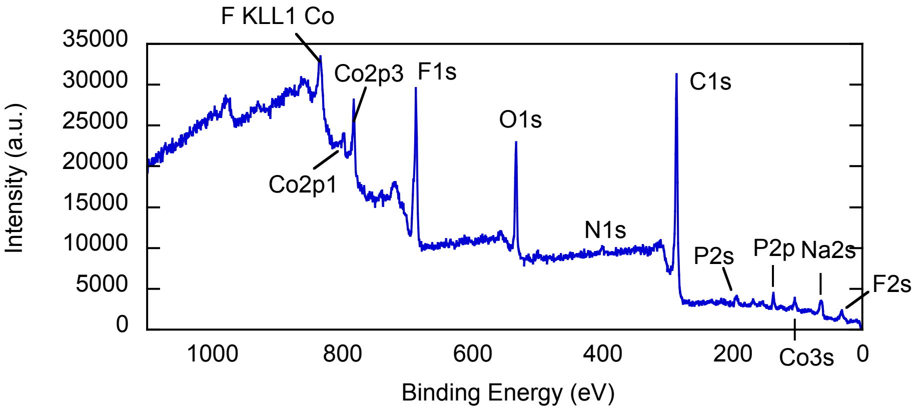

Figure 5.4. Survey XPS spectra of PMAECoCp2-CNT functionalized electrodes with PF_6^- as the counter-ion (in at% C1s 62.5%, F1s 15.5%, O1s 13%, Co2p3 3.3%, P2p 1.3%, N1s 1.2%, Na1s 0.4%, remainder, 2.9%).

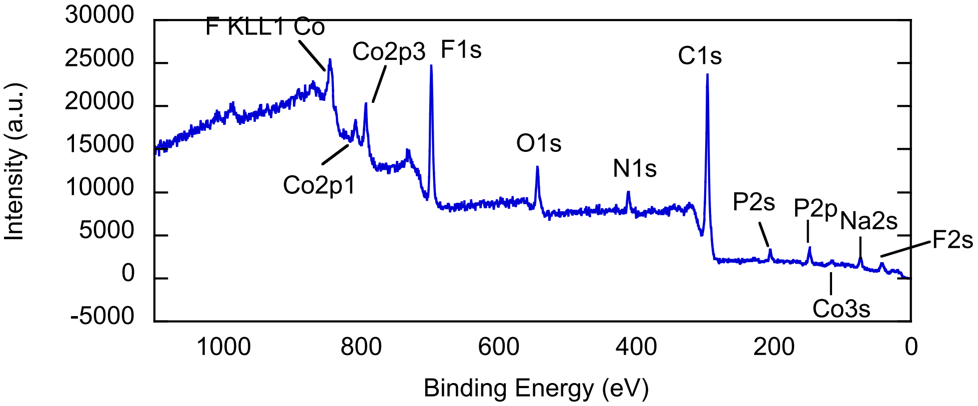

Figure 5.5. Survey XPS spectra of PMAECoCp2-monomer (in at% C1s 66.7%, F1s 16.5%, O1s 7.9%, Co2p3 2.3%, P2p 2.6%, N1s 4%).

Table S5. 1. XPS composition of $PMAECoCp_2$-CNT electrodes before and after electrochemical treatment (chronopotentiometry at +0.83 A/m^2 followed by complete discharge for -0.83 A/m^2) for 10 cycles.

Element	**At% as-synthesized (± 0.5 %)**	**At% after electrochemical treatment [from high-resolution XPS scan]**
Carbon	66.2	66.9
Oxygen	13.8	14.8
Cobalt	3.4	3.5
Fluorine (from carbon fiber support)	16.4	14.9

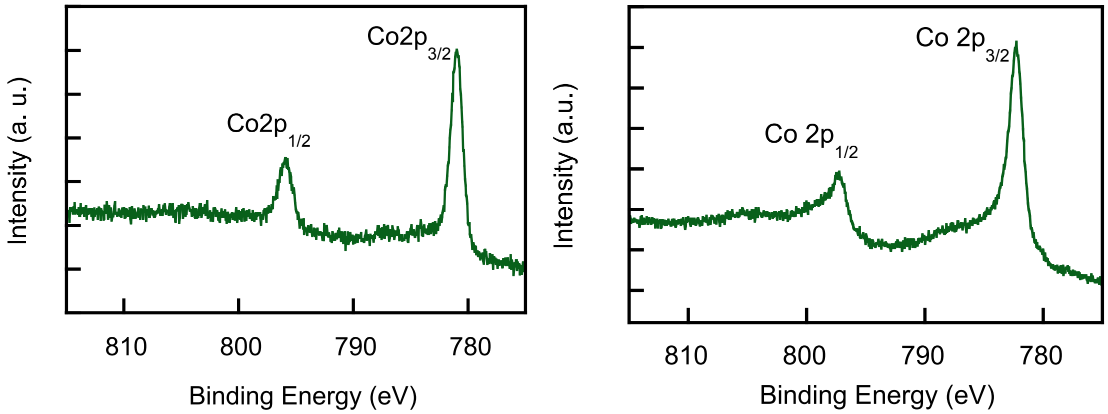

Figure 5.6. **Left.** Cobalt metal-center before reduction and ion-selective charging and discharing experiment. **Right.** Cobalt metal-center after reduction and regeneration (re-oxidation).

6. Rotating Disk Electrode

Rotating Disk Electrode. Linear sweep voltammetry experiments were performed using a BASi RDE-2 rotating disk electrode system connected to a VersaSTAT 4 potentiostat (Princeton Applied Research). The tests were conducted using 20 mL of solution in a BASi water-jacketed glass cell with a 3 mm diameter glassy carbon working electrode, a coiled platinum wire auxiliary electrode, and a silver/silver chloride reference electrode. For each run, the potential was swept from the initial potential to the final potential, and then in the reverse direction in order to revert the analyte to its original redox state. The open-circuit potentials were also obtained separately. The approach described by Laoire et al [8] was used as a guide. The concentrations of Rubpy and CpCoCb utilized were equivalent to their solubility limits in the solvents used, and were determined through nuclear magnetic resonance (NMR) spectroscopy of their saturated solutions.

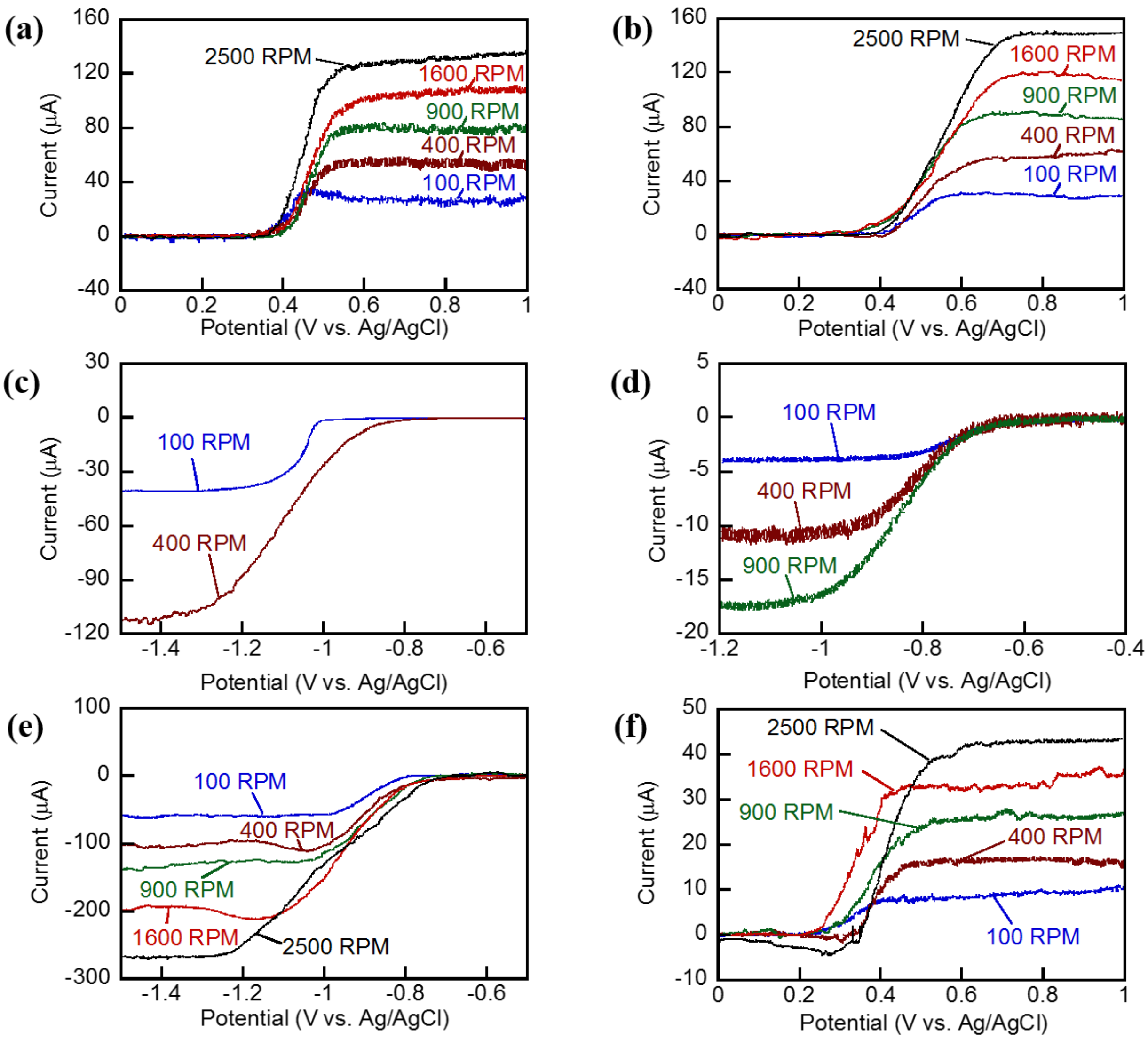

Figure 6.1. Linear sweep voltammograms (LSVs) at a scan rate of 10 mV/s for different working electrode rotation speeds. (a) 1 mM Fc, 100 mM $TBaBF_4$ in MeCN. (b) 1 mM Fc, 10 mM $TBaBF_4$ in MeCN. (c) 30 µM CpCoCb, 10 mM $TBaBF_4$ in MeCN. (d) 25 µM CpCoCb, 10 mM $TBaBF_4$ in DMSO. (e) 1 mM $CoCp_2PF_6$, 10 mM $TBaBF_4$ in MeCN. (f) 80 µM Rubpy, 10 mM $TBaBF_4$ in MeCN.

Tafel plots. The charge-transfer coefficients, α, and the standard rate constants, k^0, for each redox couple system were estimated using Tafel plots. Tafel behavior is observed in the limit of large overpotentials, and can be derived readily from the Butler-Volmer equation in the charge-transfer controlled regime [9]:

$$i_k = -i_0\left(e^{\left(\frac{-\alpha nF}{RT}\eta\right)} - e^{\left(\frac{(1-\alpha)nF}{RT}\eta\right)}\right)$$

Where i_k is the current in the absence of mass-transfer limitations, i_0 is the exchange current, η is the overpotential (defined as $E - E_{eq}$), E is the applied potential, E_{eq} is the equilibrium potential (equal to the open-circuit potential at thermodynamic equilibrium),

n is the number of electrons transferred, F is Faraday's constant, R is the gas constant, and T is the temperature.

For high overpotentials ($|\eta| \gg \frac{RT}{nF}$), the response reduces to:

$$\log|i_k| = \log i_0 + (\log e)\frac{\alpha nF}{RT}|\eta| \text{ for the cathodic branch}$$

$$\log|i_k| = \log i_0 + (\log e)\frac{(1-\alpha)nF}{RT}|\eta| \text{ for the anodic branch}$$

The slope and y-intercept of a plot of $\log|i_k|$ against $|\eta|$ reveal α and k^0, respectively. Since the Tafel relationship applies for unidirectional and totally irreversible faradaic processes, good Tafel responses are best observed when electrode kinetics are sluggish and significantly high overpotentials are applied. For the systems tested in this study, the Tafel slopes were analyzed starting at an overpotential of at leas 0.12 V, which arises from the assumption that the contribution from the backward reaction must be less than 1% of the forward reaction. For a quasireversible system, the proper selection of scan rate can also allow for the observation of irreversible behavior. A quasireversible system follows the relation suggested by Matsuda and Ayabe (1955) [10]:

$$\left|E_p - E_{p/2}\right| = \Delta(\Lambda, \alpha)\left(\frac{RT}{F}\right), \qquad \Lambda = \frac{k^0}{\left(\frac{DF}{RT}v\right)^{\frac{1}{2}}}$$

Where E_p is the peak potential, $E_{p/2}$ is the potential where the current is equal to half of the current at the peak potential, k^0 is the standard rate constant, D is the diffusivity of the redox couple species (assumed to be the same for both the oxidized and reduced species), and v is the scan rate.

For a totally irreversible system, $\Delta(\Lambda, \alpha) = \frac{1.857}{\alpha}$, and is reached for a suggested zone boundary of $\Lambda \leq 10^{-2(1+\alpha)}$. Based on order of magnitude estimates, a scan rate of 10 mV/s for the LSV tests was selected to try and meet this criterion. For each redox couple system, a Tafel plot was constructed for the LSV attained under the highest rotation speed tested. The Koutecky-Levich equation was used to correct the measured current responses from the LSVs for mass-transfer limitations:

$$i_k = \frac{i * i_l}{i_l - i}$$

Where i is the current response, and i_l is the limiting current under mass-transfer control (determined from the constant current response of the plateau portion in the LSVs at high overpotentials).

At thermodynamic equilibrium, the oxidation/reduction rate constant reduces to the standard rate constant, and the current in the absence of mass-transfer limitations reduces to the exchange current. Thus, the exchange current can be described with the following relation to yield the standard rate constant:

$$i_0 = nFAk^0C^*$$

Where A is the area of the electrode, and C^* is the bulk concentration of the analyte in solution.

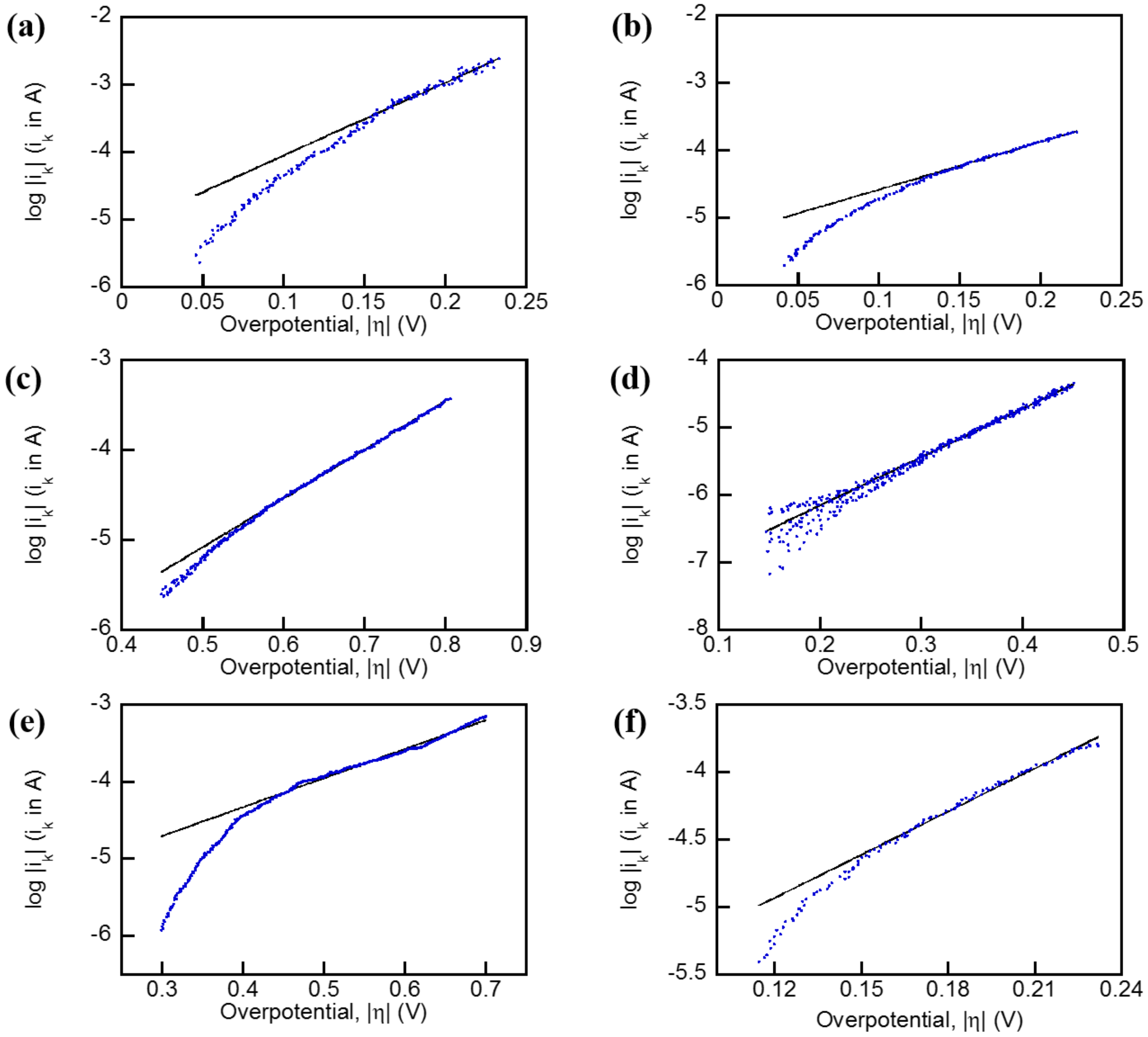

Figure 6.2. Tafel plots at a scan rate of 10 mV/s for the highest working electrode rotation speed tested. (a) 1 mM Fc, 100 mM $TBaBF_4$ in MeCN at 2500 RPM. (b) 1 mM Fc, 10 mM $TBaBF_4$ in MeCN at 2500 RPM. (c) 30 μM CpCoCb, 10 mM $TBaBF_4$ in MeCN at 400 RPM. (d) 25 μM CpCoCb, 10 mM $TBaBF_4$ in DMSO at 900 RPM. (e) 1 mM $CoCp_2PF_6$, 10 mM $TBaBF_4$ in MeCN at 2500 RPM. (f) 80 μM Rubpy, 10 mM $TBaBF_4$ in MeCN at 2500 RPM.

Table 6.1. Charge-transfer coefficients (α) and standard rate constants (k^0) for the investigated redox couple systems at the highest working electrode rotation speed tested

Redox couple system	**Open circuit potential (V vs. Ag/AgCl)**	$\boldsymbol{\alpha}$	$\boldsymbol{k^0}$ **(m/s)**
1 mM Fc, 100 mM $TBaBF_3$ in MeCN	0.32	0.36	$1.11 * 10^{-5}$
1 mM Fc, 10 mM $TBaBF_3$ in MeCN	0.35	0.58	$7.71 * 10^{-6}$
30 μM CpCoCb, 10 mM $TBaBF_3$ in MeCN	−0.39	0.32	$8.17 * 10^{-7}$
25 μM CpCoCb, 10 mM $TBaBF_3$ in DMSO	−0.45	0.42	$1.55 * 10^{-6}$
1 mM $CoCp_2PF_6$, 10 mM $TBaBF_3$ in MeCN	−0.40	0.22	$2.19 * 10^{-6}$
80 μM Rubpy, 10 mM $TBaBF_3$ in MeCN	0.25	0.37	$1.16 * 10^{-5}$

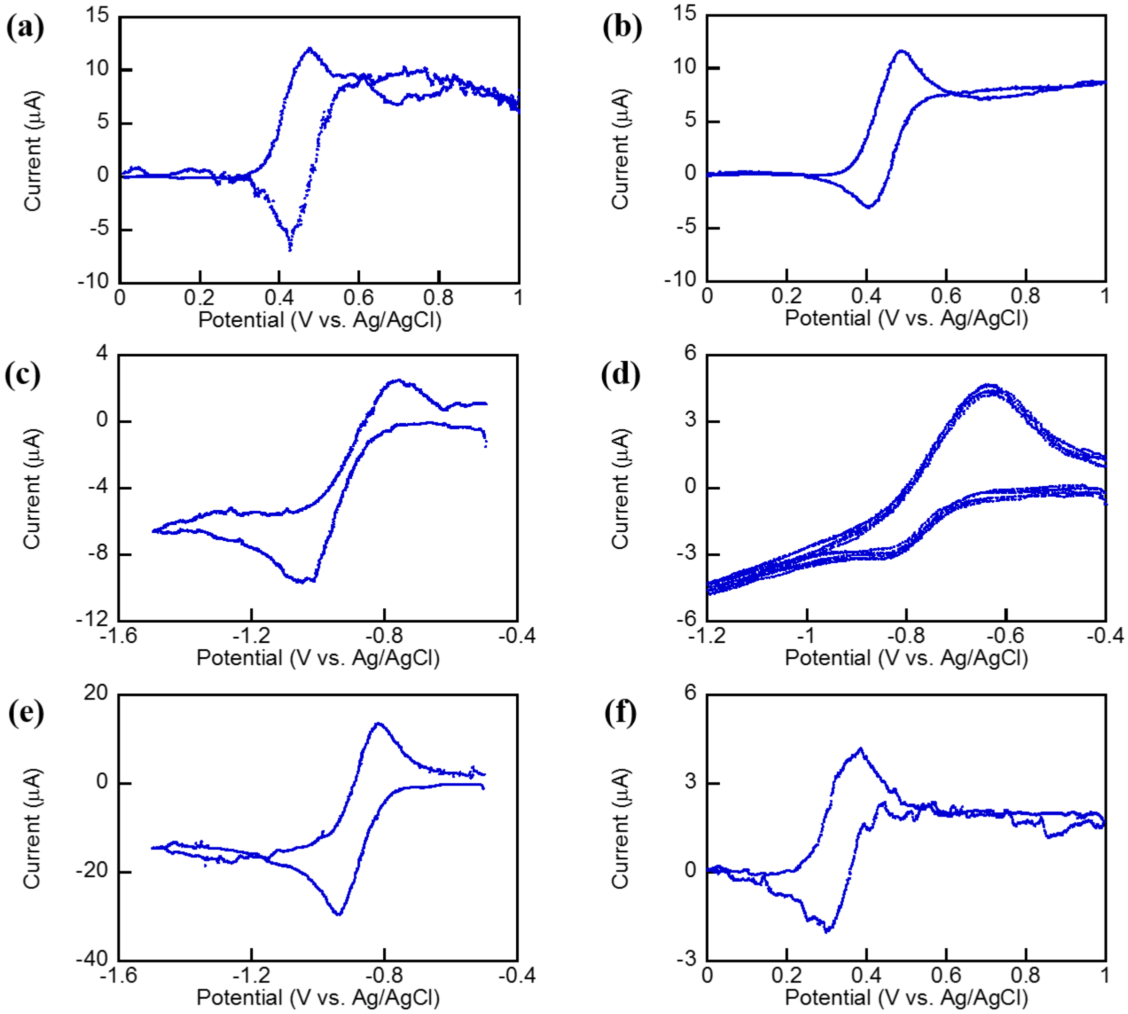

Figure 6.3. Cyclic voltammograms (CVs) at a scan rate of 10 mV/s. (a) 1 mM Fc, 100 mM $TBaBF_4$ in MeCN. (b) 1 mM Fc, 10 mM $TBaBF_4$ in MeCN. (c) 30 μM CpCoCb, 10 mM $TBaBF_4$ in MeCN. (d) 25 μM CpCoCb, 10 mM $TBaBF_4$ in DMSO. (e) 1 mM $CoCp_2PF_6$, 10 mM $TBaBF_4$ in MeCN. (f) 80 μM Rubpy, 10 mM $TBaBF_4$ in MeCN.

7. Additional Separation Data

Liquid measurements. The uptake of organic anions to the electrodes was estimated by running electrochemical separations in deuterated water (D_2O) and analyzing the liquid samples before and after by NMR, or UV-vis spectophotometer. The amount adsorbed onto the electrode is calculated based on the difference between the integrated areas of the peaks of the compounds, ($c_{initial}$-c_{final}) x volume, with respect to an external reference as the standard (naphthalene in organic solvent, 3-(trimethylsilyl)-1-propanesulfonic acid in aqueous). All electrochemical studies were performed on a VersaSTAT 4 potentiostat (Princeton Applied Research) with automatic IR compensation between 50 MΩ and 5 Ω. For in-situ measurements, asymmetric electrodes were placed in a UV-vis quartz vial, with an electrode distancing of 1 cm between and the purged with nitrogen. The measurements were obtained at the peak absorbance wavelength (280 nm) for the aromatic molecules.

Gas-phase measurements. Electrochemical reactions were performed in a gas tight three-electrode cell under N_2 atmosphere flowing continuously at 20 mL/min, with electrodes of the same dimensions as those for the pH test. The gas concentrations were measured on an Agilent 7890 GC system equipped with two HP-PLOT/Q columns and an HP-PLOT Molesieve column in series to perform the chromatographic separations. A thermal conductivity detector (TCD) was used to measure the output signals of the hydrogen, oxygen, and nitrogen relative to the Argon carrier gas. Gas samples were pulled and analyzed by the GC system approximately every 12 minutes.

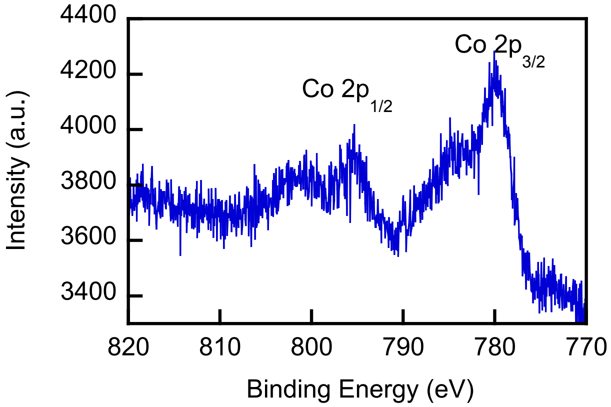

Figure 7.1. High-resolution XPS of cobalt in PCoCpCbMA.

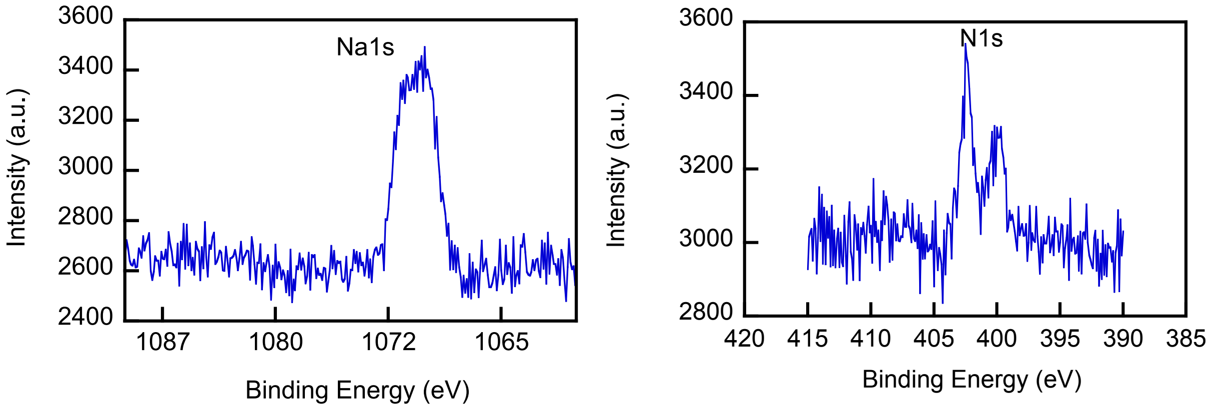

Figure 7.2. High-res XPS of Na1s vs N1s of butyl pyridinium adsorbed on PCoCpCbMA-CNT electrode.

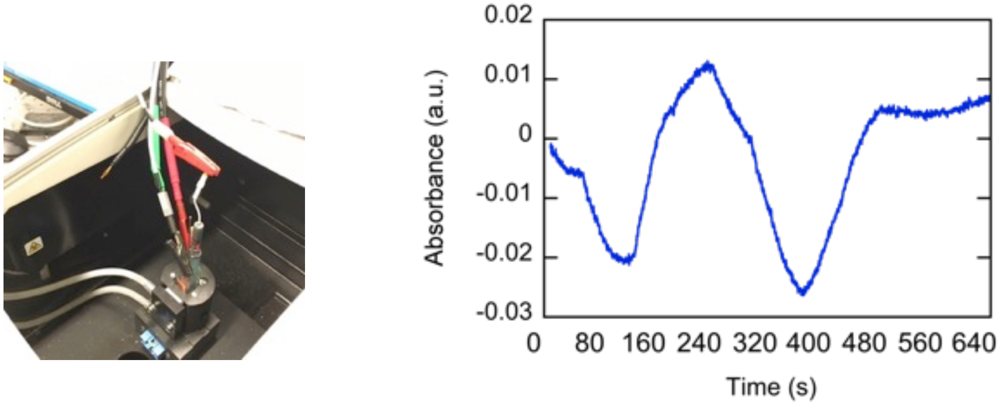

Figure 7.3. Reversible adsorption of butyl-pyridinium (300 uM But-pyr with 100 mM $NaClO_4$) under potential using PCoCpCbMA-CNT//PVF-CNT. Adsorption under -0.7 V and desorption under 0 V.

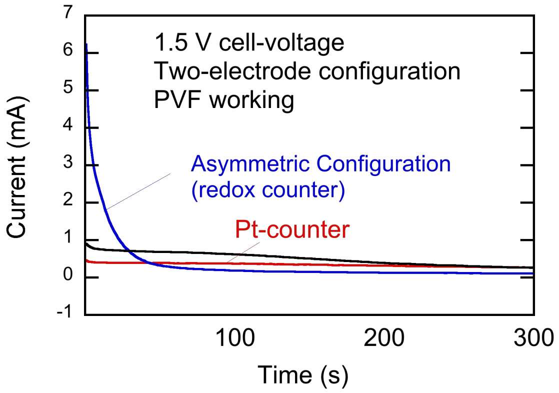

Figure 7.4. Chronoamperometry at 1.5 V of various configurations of PVF-CNT with various counters. Charging is much more significant with the asymmetric electrode counter $PMMAECoCp_2$-CNT.

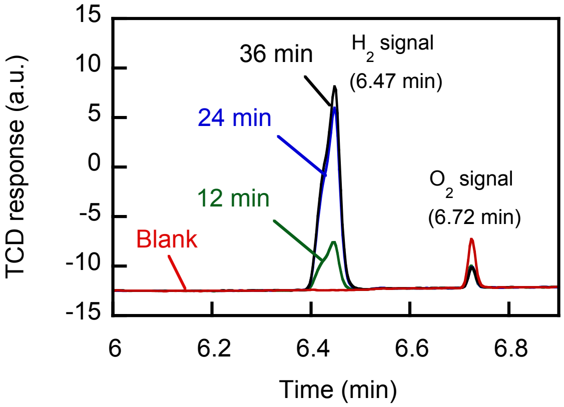

Figure 7.5. GC-measurements of headspace of PVF-CNT//Pt system with time (sampling time every 12 min). Note that the O_2 content decreases slightly due to purging when compared to blank, with the O_2 being trace amounts from the carrier gas. The H_2 concentration at 12 min ~ 122 ppm, at 24 min ~463 ppm and at 36 min ~520 ppm.

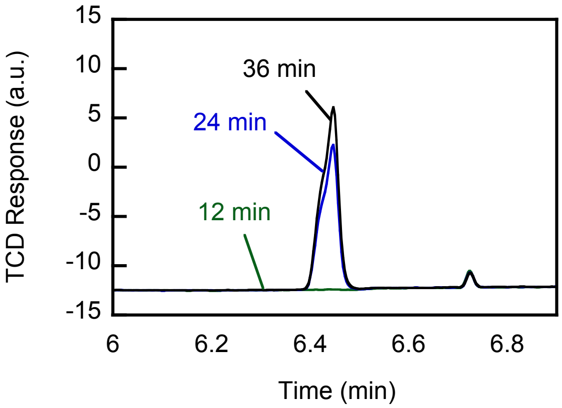

Figure 7.6. GC-measurements of headspace of PVF-CNT//PMAECoCp₂ system with time (sampling time every 12 min). After 24 min the H_2 concentration climbs due to the asymmetric cell being fully charged, yet during the initial period of chronopotentiometry of 600 s the H_2 is fully suppressed.

References

1. MacFarland, D.K. & Gorodetzer, R. Rotor-shaped cyclopentadienyltetraphenylcyclobutadienecobalt - An advanced inorganic experiment. *Journal of Chemical Education* **82**, 109-110 (2005).
2. Mao, X.W., Simeon, F., Achilleos, D.S., Rutledge, G.C. & Hatton, T.A. Metallocene/carbon hybrids prepared by a solution process for

supercapacitor applications. *Journal of Materials Chemistry A* **1**, 13120-13127 (2013).

3. Su, X., Kulik, H., Jamison, T.F. & Hatton, T.A. Anion-selective redox-electrodes: electrochemically-mediated separation with heterogeneous organometallic interfaces. *Advanced Functional Materials* (2016).
4. Ren, L.X. et al. Preparation of Side-Chain 18-e Cobaltocenium-Containing Acrylate Monomers and Polymers. *Macromolecules* **43**, 9304-9310 (2010).
5. Ren, L.X., Hardy, C.G. & Tang, C.B. Synthesis and Solution Self-Assembly of Side-Chain Cobaltocenium-Containing Block Copolymers. *J Am Chem Soc* **132**, 8874-+ (2010).
6. Sheats, J.E. & Rausch, M.D. Synthesis and properties of cobaltocinium salts. 1. Synthesis of monosubstituted cobaltocinium salts. *Journal of Organic Chemistry* **35**, 3245-& (1970).
7. Ruttiger, C. et al. One for all: cobalt-containing polymethacrylates for magnetic ceramics, block copolymerization, unexpected electrochemistry, and stimuli-responsiveness. *Polymer Chemistry* **7**, 1129-1137 (2016).
8. Laoire, C.O., Plichta, E., Hendrickson, M., Mukerjee, S. & Abraham, K.M. Electrochemical studies of ferrocene in a lithium ion conducting organic carbonate electrolyte. *Electrochim Acta* **54**, 6560-6564 (2009).
9. Bard, A.J. & Faulkner, L.R. Electrochemical Methods: Fundamentals and Applications, Edn. 2nd. (Wiley, 2000).
10. Matsuda, H. & Ayabe, Y. Zur Theorie Der Randles-Sevcikschen Kathodenstreahl-polarographie. *Zeitschrift Fur Elektrochemie* **59**, 494-503 (1955).